Journal of Medicinal Chemistry

ARTICLE

pubs.acs.org/jmc

5-Benzamidoisoquinolin-1-ones and 5-(ω-Carboxyalkyl)isoquinolin-1-ones as Isoform-Selective Inhibitors of Poly(ADP-ribose) Polymerase 2 (PARP-2)

Peter T. Sunderland,[†] Esther C. Y. Woon,[†,∥] Archana Dhami,[†] Aoife B. Bergin,[†,⊥] Mary F. Mahon,[‡] Pauline J. Wood,[†] Louise A. Jones,[§] Sophie R. Tully,[§] Matthew D. Lloyd,[†] Andrew S. Thompson,[†] Hashim Javaid,[§] Niall M. B. Martin,[§] and Michael D. Threadgill*[,†]

[†]Medicinal Chemistry, Department of Pharmacy and Pharmacology, University of Bath, Claverton Down, Bath BA2 7AY, U.K.

[‡]Crystallography Unit, Department of Chemistry, University of Bath, Claverton Down, Bath BA2 7AY, U.K.

[§]KuDOS Pharmaceuticals Ltd., 410 Cambridge Science Park, Milton Road, Cambridge CB4 0PE, U.K.

Supporting Information

ABSTRACT: PARP-2 is a member of the poly(ADP-ribose) polymerase family, with some activities similar to those of PARP-1 but with other distinct roles. Two series of isoquinolin-1-ones were designed, synthesized, and evaluated as selective inhibitors of PARP-2, using the structures of the catalytic sites of the isoforms. A new efficient synthesis of 5-aminoisoquinolin-1-one was developed, and acylation with acyl chlorides gave 5-acylaminoisoquinolin-1-ones. By examination of isoquinolin-1-ones with carboxylates tethered to the 5-position, Heck coupling of 5-iodoisoquinolin-1-one furnished the 5-CH=CHCO$_2$H compound for reduction to the 5-propanoic acid. Alkylation of 5-aminoisoquinolin-1-one under mildly basic conditions, followed by hydrolysis, gave 5-(carboxymethylamino)isoquinolin-1-one, whereas it was alkylated at 2-N with methyl propenoate and strong base. Compounds were assayed in vitro for inhibition of PARP-1 and PARP-2, using FlashPlate and solution-phase assays, respectively. The 5-benzamidoisoquinolin-1-ones were more selective for inhibition of PARP-2, whereas the 5-(ω-carboxyalkyl)isoquinolin-1-ones were less so. 5-Benzamidoisoquinolin-1-one is the most PARP-2-selective compound ($IC_{50(PARP-1)}/IC_{50(PARP-2)}$ = 9.3) to date, in a comparative study.

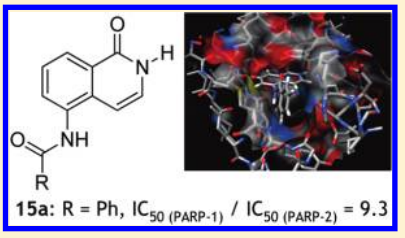

INTRODUCTION

Poly(ADP-ribosyl)ation of proteins, first reported in 1963,[1] involves the transfer of multiple ADP-ribose units from substrate NAD^+ onto glutamate residues of the target proteins, resulting in the formation of polyanionic poly(ADP-ribose) (PAR) polymers. There has been much research effort since to characterize the structures and functions of the poly(ADP-ribose) polymerases (PARPs), the family of enzymes responsible for catalysis of this reaction.[2−5]

PARP-1 is responsible for most of the poly(ADP-ribosyl)ation activity in the cell and has a major role in regulating the repair of damaged DNA. It is a 116 kDa protein with three major domains: an N-terminal DNA-binding domain carrying three zinc fingers,[6] a central automodification domain (containing also a nuclear localization signal[7] and sites for cleavage by caspase-3[8]), and a C-terminal NAD^+-binding catalytic domain. The catalytic activity of the PARP-1 is activated by detection of a damaged site, and PAR is built up on histone-1 and on PARP-1 itself. Inhibition of PARP-1 therefore inhibits repair of damaged DNA, and several inhibitors of this enzyme are currently in clinical trial as sensitizers to the effects of cytotoxic DNA-damaging drugs in several tumors and as single-agent therapies in BRCA-mutant breast cancer.[9−14] In addition to its role in regulating repair of damaged DNA, PARP-1 also regulates NF-κB and processes and molecules downstream therefrom. Thus, inhibitors of the catalytic activity of PARP-1 have shown interesting activity in vivo in models of several disease states, including hemorrhagic shock, myocardial infarction, stroke, and other ischemia−reperfusion injuries, as well as in inflammatory disorders and reproductive health.[15−20] Recently, inhibitors of PARP-1 have also been shown to inhibit angiogenesis and metastasis in cancer.[21−23]

PARP-2 is a 62 kDa protein with three functional domains.[24] The N-terminal DNA-binding domain lacks zinc fingers but is rich in basic amino acids, which account for the binding to DNA. The differences in structure of the DNA-binding domains of PARPs 1 and 2 may also reflect the differences in the DNA structures which the two enzymes recognize and the fact that PARP-2 binds to single-strand breaks (SSBs) less efficiently than does PARP-1. The automodification domain is also responsible for the protein−protein interactions that PARP-2 shares with various partners, including PARP-1, XRCC1, and DNA ligase 3.[25] The catalytic domains of mouse and human PARP-2 are highly conserved, and both show high homology with the human PARP-1 catalytic domain (69% in the case of human PARP-2).[24]

Received: August 23, 2010
Published: March 18, 2011

dx.doi.org/10.1021/jm1010918 | J. Med. Chem. 2011, 54, 2049–2059

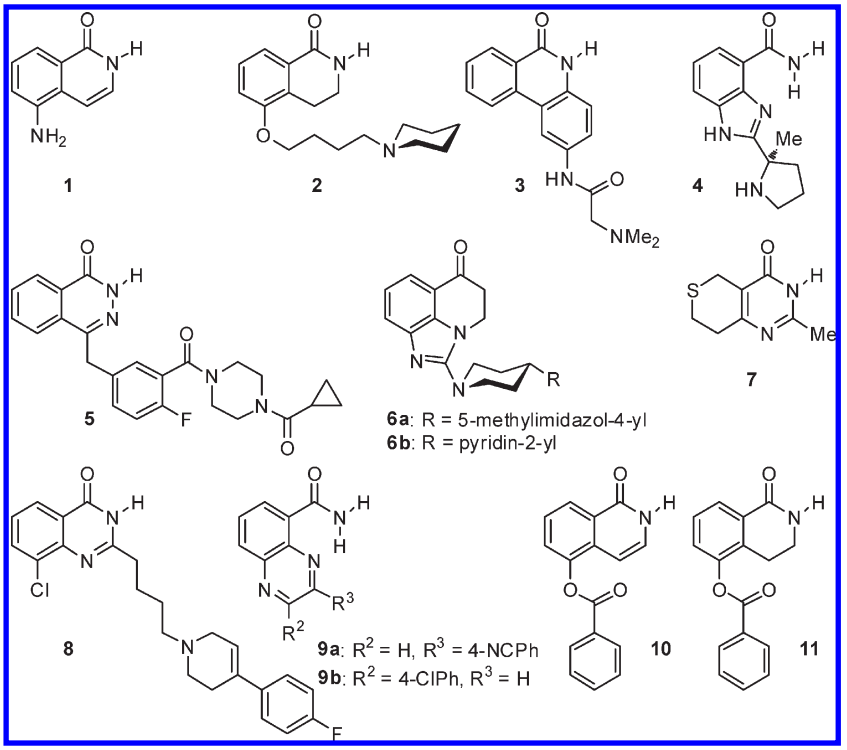

Figure 1. Structures of reported potent non-isoform-selective inhibitors **1**−**7**, PARP-1-selective inhibitor **8**, and PARP-2-selective inhibitors **9**−**11**.

This isoform accounts for approximately 5−10% of the total cellular PARP activity.[25] It can heterodimerize with PARP-1, and it shares many functions and targets. However, PARP-2 has some different protein targets and potential functions. Schreiber et al.[25] showed that PARP-2$^{-/-}$ mouse embryonic fibroblasts have delayed repair of alkylated bases in DNA following treatment with *N*-methyl-*N*-nitrosourea (MNU) and suggest that the PARP-1/PARP-2 heterodimer is important for efficient base-excision repair. By contrast, Fisher et al.[26] found that a reduction in PARP-1 significantly reduced the rate of repair of single-strand breaks in DNA but reduction in PARP-2 had only a minor effect. PARP-2 interacts with TRF2,[27] a telomere-binding regulatory protein, and affects its ability to bind to DNA both through a noncovalent interaction of PAR with the DNA-binding domain of TRF2 and through a covalent modification at the dimerization domain. PARP-2 may have a functional role in the maintenance of telomeres, but further work using selective inhibitors of this isoform is required to gain insights into the precise molecular mechanisms at work. Antisense knockdown of PARP-2 in a mouse model of colitis resulted in improvement in inflammation and normalization of colonic function.[28] Deletion of PARP-2 but not of PARP-1 leads to a significant diminution in $CD4^+CD8^+$ double-positive thymocytes,[29] suggesting that PARP-2 has a role in survival of T-cells during thymopoiesis and may regulate the apoptosis of thymocytes. PARP-2 is widely expressed in the seminiferous epithelium, in contrast to limitation of PARP-1 to the peripheral cell layer,[25,30] pointing to distinct roles in spermatogenesis and a more prominent role for PARP-2. PARP-2 knockout mice display lipodystrophy,[31] probably due to regulation of the expression of peroxisome proliferator-activated receptor-γ by PARP-2. These roles for PARP-2, which are distinct from those of the major isoform PARP-1,[32] point to the need for selective inhibitors initially as pharmacological tools to help resolve and distinguish the roles of PARP-2 but also, in the longer term, possibly as drugs.

Most attempts to identify PARP-2-selective inhibitors have relied on screening libraries of inhibitors of PARP-1 against both isoforms. Interestingly, most of the clinical candidate PARP-1 inhibitors and of the widely used pharmacological tool inhibitors display little or no selectivity, and thus, any pharmacological effect thereof must be regarded as the effect of pan-PARP inhibition or, at minimum, of PARP-1 and PARP-2 together. As shown in this paper, our lead PARP-1 inhibitor 5-aminoisoquinolin-1-one **1** (5-AIQ, Figure 1), which is potently active in vivo,[15,17−20,23] is devoid of isoform selectivity in vitro. Similarly, two other standard PARP-1 inhibitors, DPQ **2** and PJ34 **3**, are reported to have little isoform-selectivity between PARP-1 and PARP-2.[33] The latest clinical candidates veliparib **4**[34] and olaparib **5**,[36] the biochemical tools BYK49187 **6a**,[35] BYK236864 **6b**[35] and the thiopyranopyrimidinone **7**[37] also inhibit the two isoforms potently but approximately equally. However, in 2006, Ishida et al. reported the identification of a series of quinazolin-4-ones as selective inhibitors of PARP-1, of which **8** was the most selective, with $IC_{50(PARP\text{-}1)}$ = 13 nM and $IC_{50(PARP\text{-}2)}$ = 500 nM (selectivity ratio of 39); minor modifications to the substitution on the fluorophenyl ring were tolerated in the structure−activity relationship (SAR), but the long pendant 3-(4-aryl-1,2,5,6-tetrahydropyridin-1-yl)propyl group at the 3-position of the quinazolinone was shown to be essential in this series, as 5-chloro-2-methylquinazolin-4-one was non-isoform-selective and was 92-fold less active against PARP-1 than was **8**.[38] The same paper also reports that **9a** was some 12-fold more potent as an inhibitor of PARP-2 than it was of PARP-1; other varied substituents in the 4-position of the phenyl were tolerated with little loss of selectivity.[38] The observed selectivities were rationalized by examining X-ray structures of cocrystals of

dx.doi.org/10.1021/jm1010918 |*J. Med. Chem.* 2011, 54, 2049–2059

Scheme 1. New Efficient Synthesis of 1 and Synthesis of 5-(Acylamino)isoquinolin-1-ones 15a−n[a]

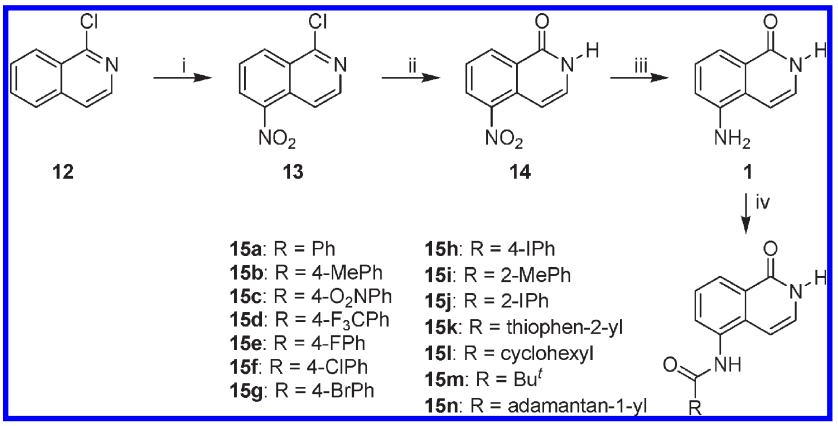

[a] Reagents and conditions: (i) HNO_3, H_2SO_4, 0°C, 92%; (ii) AcOH, 100°C, 82%; (iii) H_2, Pd/C, EtOH, aq HCl, 66%; (iv) RCOCl, pyridine, 90 °C, 86% (**15a**), 82% (**15b**), 71% (**15c**), 72% (**15d**), 68% (**15e**), 77% (**15f**), 81% (**15g**), 76% (**15h**), 63% (**15i**), 61% (**15j**), 51% (**15k**), 68% (**15l**), 68% (**15m**), 59% (**15n**).

PARP-1 with inhibitors and of homology models of PARP-2. Separately, this group also reported that a 2-arylquinoxaline-5-carboxamide **9b** had 5-fold selectivity for inhibition of PARP-2.[39] By far the most selective inhibitors of PARP-2 claimed to date are a series of 5-benzoyloxyisoquinolin-1-ones, 5-phenacyloxyisoquinolin-1-ones, and 3,4-dihydroisoquinolin-1-ones, of which **10** and **11** appear to show 60-fold and 16-fold selectivity, respectively.[33] These compounds, which pick up the usual PARP-binding contacts of the classical (3,4-dihydro) isoquinolin-1-one pharmacophore, achieve their selectivity by relatively weak micromolar binding to PARP-1 rather than great potency against PARP-2. This poor binding to PARP-1 is probably due to the 5-benzoyloxy and 5-phenacyloxy substituents being too large to be accommodated in the slightly smaller hydrophobic binding pocket of PARP-1, compared to that of PARP-2 (see below).

In the present work, we report on two different approaches to the discovery of PARP-2-selective inhibitors, both based on the isoquinolin-1-one core which gives good binding to both isoforms through the hydrogen-bonding network to the lactam oxygen and N−H and through π-stacking of the aromatic ring to the adjacent Tyr residues (Tyr^{907}/Tyr^{449}).

CHEMICAL SYNTHESIS

Noting the remarkable selectivity for inhibition of PARP-2 by **10** claimed by Pellicciari et al.,[33] we sought to use this core to develop further selective inhibitors of this isoform. Inhibitors **10** and **11** both contain *O*-aryl esters, which are likely to be labile to hydrolysis in physiological media. To obviate this potential problem, the ester was replaced by an amide in target compound **15a** (Scheme 1); this amide should be isosteric but may restrict rotation in this part of the molecule.

Synthesis of **15a** and its analogues **15b−n** required quantities of **1**. This compound is commercially available but is prohibitively expensive for applications in synthesis. There are three previous published syntheses of **1** (where the critical steps are a Polonowski rearrangement 5-nitroisoquinoline *N*-oxide,[40] reductive cyclization of methyl 2-cyanomethyl-3-nitrobenzoate,[41] and condensation of methyl 2-methyl-3-nitrobenzoate with dimethylformamide dimethylacetal[15]), but all have severe limitations. Thus, for large-scale preparation of **1**, a new synthesis was needed with requirements for high yield and avoidance of scale-limiting steps such as column chromatography. Scheme 1 shows our development of this important new route. In this route, the 5-nitrogen substituent is introduced by nitration. However, the most nucleophilic position of isoquinolin-1-ones is 4-C,[42] so direct nitration of isoquinolin-1-one was not feasible. The activating enamide function of isoquinolin-1-one was masked as the iminochloride in **12**. Commercially available 1-chloroisoquinoline **12** was nitrated selectively in the 5-position in 92% yield. To achieve this regioselectivity, it was necessary to predissolve **12** in concentrated sulfuric acid to ensure that the heterocyclic ring was fully protonated and deactivated before addition of the nitrating reagents. The iminochloride in **13** was hydrolyzed by heating in acetic acid to provide **14** in high yield, and catalytic hydrogenation of the nitro group, under conditions previously reported,[42] then furnished **1**. This new sequence is reliable, high-yielding (54% overall), and highly reproducible and involves only two intermediate recrystallizations and no chromatography for purification, giving the potential for it to be used on larger scales.

5-Benzamidoisoquinolin-1-one **15a** was synthesized in good yield by acylation of **1** with benzoyl chloride in hot pyridine (Scheme 1); the relatively forcing conditions were required to overcome the poor nucleophilicity of the exocyclic amine in **1** and to ensure good solubility. To explore the structure−activity relationships around this phenyl ring, a series of 5-(substituted benzamido)isoquinolin-1-ones **15b−j** were prepared similarly from **1** and substituted benzoyl chlorides. Following a classical medicinal chemical replacement of the benzene aromatic ring with thiophene led to design of 5-(thiophen-2-ylcarboxamido)isoquinolin-1-one **15k**, which was prepared from **1** with thiophene-2-carbonyl chloride. The need for aromaticity was tested by replacement with cyclohexyl in **15l** and by 3D bulky aliphatic groups in the pivalamido analogue **15m** and the adamantylcarboxamido compound **15n**.

Compound **22** (Scheme 2) extends the structure of **15a** by introducing a methyl group at the 3-position of the isoquinolin-1-one ring system. The synthesis of this target was analogous to that of **15a**, thus requiring 3-methylisoquinolin-1-one **21** as a starting material. As for **1**, this educt is commercially available but prohibitively expensive (>£5000 g^{-1}). None of the synthetic sequences to **1** could be adapted to the 3-methyl analogue **21**;

dx.doi.org/10.1021/jm1010918 |*J. Med. Chem.* 2011, 54, 2049–2059

Scheme 2. Synthesis of 5-Benzamido-3-methylisoquinolin-1-one 22[a]

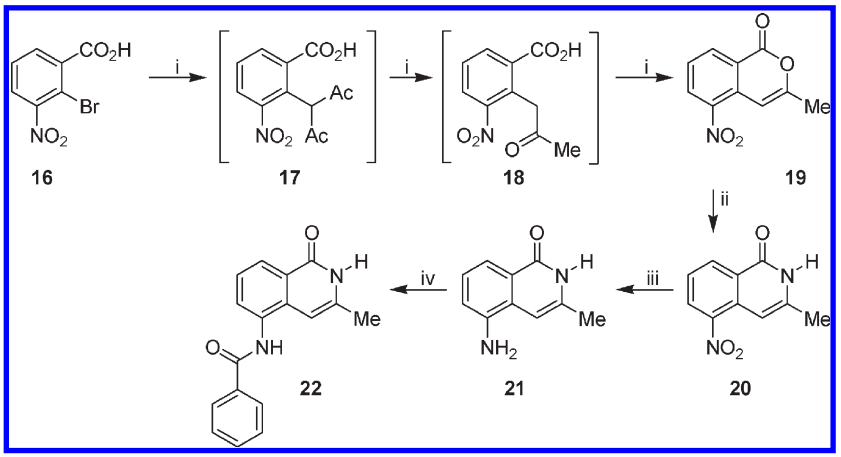

[a] Reagents and conditions: (i) pentane-2,4-dione, KO^{t}Bu, Cu, ^{t}BuOH, reflux, 23%; (ii) NH_3, $MeO(CH_2)_2OH$, reflux, 68%; (iii) $SnCl_2$, EtOH, 70°C, 59%; (iv) PhCOCl, pyridine, 90 °C, 72%.

reaction of methyl 2-methyl-3-nitrobenzoate with dimethylacetamide dimethylacetal gives 3-dimethylamino-1-methoxy-5-nitronaphthalene rather than **19**,[43] and 1-chloro-3-methyl-5-nitroisoquinoline is only available by a low-yielding Polonowski rearrangement of 3-methyl-5-nitroisoquinoline *N*-oxide.[44] A new route was required, starting from a suitable 1,2,3-trisubstituted benzene. The Hurtley reaction involves Cu-catalyzed displacement of the bromine of *o*-bromobenzoic acids by the enolates of β-diketones.[45,46] However, we have previously shown that the reaction fails with 3-bromo-2-nitrothiophene-4-carboxylic acid.[47] Despite this adverse omen, 2-bromo-3-nitrobenzoic acid **16** did react with the potassium enolate of pentane-2,4-dione in the presence of Cu powder. Under the reaction conditions (boiling *tert*-butanol), the immediate Hurtley coupling product **17** was not observed; rather it was deacetylated to the monoketone **18**, which cyclized to give the isocoumarin **19**, achieving several synthetic steps in one pot. The isocoumarin **19** was converted to the isoquinolin-1-one **20**, and reduction of the nitro group with tin(II) chloride furnished the required intermediate **21** for acylation to provide the target amide **22**.

In 2004, the crystal structure of the catalytic fragment of murine PARP-2 was solved[48] at 2.8 Å resolution, 7 years after the data for the chicken PARP-1 catalytic fragment were made available.[49] The high degree of homology of the PARP catalytic domain between different species means that PARP inhibitors are unlikely to show a wide species difference in their binding of inhibitors between chicken, mouse, and human PARPs, for a specific isoform. The binding of inhibitors to PARP-1 was deduced by Ruf et al.[50] to be due to hydrogen bonding from the carbonyl of lactams/amides in the inhibitors to Gly^{863}-NH and Ser^{904}-OH and from the lactam/amide N−H to Gly^{863}-O and hydrophobic or π-stacking interactions with Tyr^{907}. PARP-2 is a much smaller protein than is PARP-1, but the hydrogen-bonding and π-stacking motifs are retained in the nicotinamide-binding site, with Gly^{405} (PARP-2) corresponding to Gly^{863} (PARP-1), Ser^{446} (PARP-2) corresponding to Ser^{904} (PARP-1), and Tyr^{449} (PARP-2) corresponding to Tyr^{907} (PARP-1). Our inspection of the binding sites of the isoforms noted that Gln^{763} (neutral, polar) in PARP-1 is replaced by Lys^{308} (basic, polar); these residues are located slightly above the plane of the nicotinamide mimic and at the edge of the hydrophobic pocket, i.e. "south" of the 5-position of potentially bound isoquinoline-1-ones. By use of molecular modeling to design further potentially selective inhibitors, the crystal structures of chicken PARP-1 with 8-hydroxy-2-methylquinazolin-4-one bound[50] and murine PARP-2[48] were used as starting structures, from which the binding pockets were established and compared. The binding pocket of PARP-1 was measured and mapped, together with key interactions between the bound inhibitor and the pocket. Comparisons were also made to PARP-1 without inhibitor to confirm that the receptor binding pocket is relatively rigid and does not change conformation upon binding the substrate or an inhibitor ligand. The distances observed in PARP-1 were then used to dock a minimized and charged (Gastieger/Hückel) structure of **1** into the binding pocket of PARP-2. Once docked, restraints were added (as observed in the PARP-1 model) and the ligand was subjected to molecular dynamics (300 K for 5 ps) and then reminimized. The ligand and binding pocket (5.0 Å from ligand) were then subjected to molecular dynamics (300 K for 5 ps), and the complete complex (enzyme and **1**) was minimized to give the final model. In this model, the basic Lys^{308} sat close (3.1 Å) to the 5-amine of **1**. Two short series of compounds were designed to exploit this opportunity for isoform-selectivity by linking an anionic carboxylate to the 5-position of the isoquinolin-1-one.

In the first three compounds, the carboxylic acid was attached to the 5-position of the isoquinolin-1-one through all-carbon links (Scheme 3). Compound **24** was prepared by hydrolysis of 5-cyanoisoquinolin-1-one **23**.[51,52] The targets **26** and **27** have a C_2 chain between the carboxylic acid and the isoquinoline, the former with a rigid link and the latter with a flexible link. These were approached by a Heck coupling of 5-iodoisoquinolin-1-one **25** to give **26**.[52] Selective hydrogenation of the exocyclic double bond under acidic conditions led to **27**.

Exploiting the now ready availability of **1** as a starting material, it was planned to attach carboxylic acids through linkers to the exocyclic amine to provide target compounds such as **29** (Scheme 4). Heating **1** with ethyl bromoacetate in DMF in the presence of tertiary amine base alkylated the weakly nucleophilic amine, giving the ester **28** in modest yield. Hydrolysis then furnished the carboxylic acid **29**. In an attempt to access the homologous ester **30**, **1** was treated with sodium hydride and

dx.doi.org/10.1021/jm1010918 |*J. Med. Chem.* 2011, 54, 2049–2059

Scheme 3. Synthesis of C-Linked 1-Oxoisoquinoline-5-carboxylic Acids 24, 26, and 27[a]

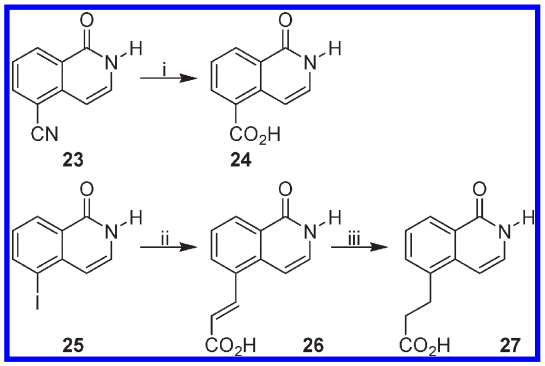

[a] Reagents and conditions: (i) KOH, EtOH, reflux, then aq HCl, 83%; (ii) $HO_2CCH{=}CH_2$, $Pd(OAc)_2$, Et_3N, EtCN, reflux, 97%; (iii) H_2, Pd/C, EtOH, 66%.

Scheme 4. Synthesis of 5-(ω-Carboxyalkylamino)-isoquinolin-1-ones 29 and 32[a]

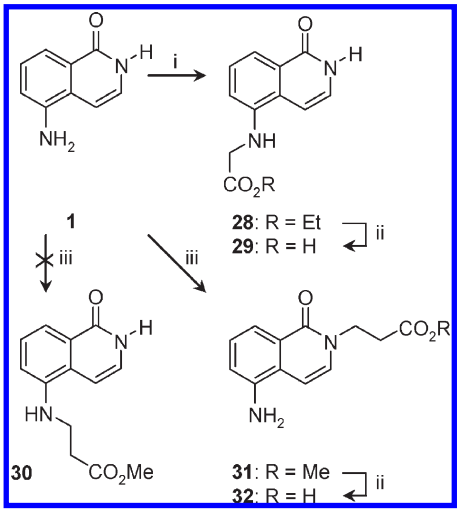

[a] Reagents and conditions: (i) EtO_2CCH_2Br, $^iPr_2NEt$, NaI, DMF, 80°C, 19%; (ii) aq HCl, reflux, 87% (**29**), 85% (**32**); (iii) NaH, THF, $MeO_2CCH{=}CH_2$, 67%.

methyl acrylate. Surprisingly, the sole isolable product was **31**, where the $CH_2CH_2CO_2Me$ unit is attached to the lactam 2-N, rather than the exocyclic amine. The location of this unit was confirmed by the ^{1}H NMR chemical shift of the NCH_2 protons (δ 4.09, more typical of CH_2 attached to the lactam rather than CH_2 attached to an aniline nitrogen) and by HMBC correlations between these CH_2 protons and the lactam carbonyl-^{13}C at δ 161.2 and between these CH_2 protons and 3-C at δ 130.6; these correlations are incompatible with the alternatives **30** or 1-($MeO_2CH_2CH_2CO$)-5-NH_2-isoquinoline (from alkylation at oxygen). Sodium hydride is a much stronger base than the diisopropylethylamine used in the synthesis of **28** and is capable of removing the lactam N−H proton. In the anion so generated, the N^- of the lactam is more nucleophilic than the neutral exocyclic NH_2 and reacts with the electrophile. Anions derived from other 5-substituted isoquinolin-1-ones usually react through the 2-N with alkylating electrophiles,[42,53,54] although there are some examples of reaction at the exocyclic oxygen at the

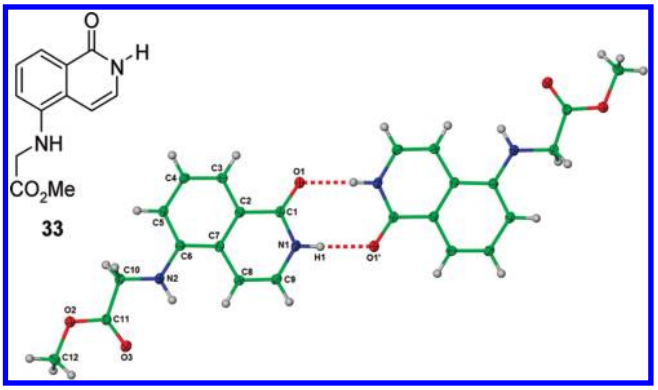

Figure 2. X-ray crystal structure of methyl ester **33**, showing the hydrogen-bonded pairs in the crystal. Ellipsoids are represented at 30% probability, and O1′ is related to O1 by the $1 - x$, $1 - y$, $3 - z$ symmetry operation.

1-position under Mitsunobu conditions.[52] Hydrolysis of the ester of **31** with aqueous acid gave the corresponding carboxylic acid **32**.

In view of the unexpected regioselectivity of the reaction of **1** with methyl propenoate under strongly basic conditions, it was necessary to prove the structure of **28** or **29** through an X-ray crystal structure determination. Careful recrystallization of the carboxylic acid **29** from methanol provided diffraction-quality crystals of the corresponding methyl ester **33**. The crystal structure (Figure 2) confirmed the expected structure, with the CH_2CO_2Me attached to the exocyclic amine. The isoquinolin-1-ones formed hydrogen-bonded pairs in the crystal, with the lactam N−H bonded to the carbonyl oxygen of the partner molecule. The 5-$NHCH_2CO_2Me$ unit adopted an extended conformation but appears not to be hydrogen-bonded; the exocyclic nitrogen was planar, as expected, and the methylene was orientated away from the peri 4-H.

BIOCHEMICAL AND CELL BIOLOGICAL EVALUATION

The two series of 5-substituted isoquinolin-1-ones were evaluated in vitro for inhibition of the catalytic activities of full-length active human PARP-1 isolated from HeLa cell nuclear extract (using a FlashPlate assay previously developed by us[55]) and full-length mouse PARP-2 (using a solution-phase assay); the results are presented in Table 1 for **15a**−**n**, **22**, **24**, **26**, **27**, **29**, and **32**. **1** and the two claimed PARP-2-selective inhibitors **9b**[38] and **10**[33] from the literature were assayed as controls.

As expected, **1** showed no selectivity toward either isoform, with $IC_{50} \approx 1$ μM for each. The 5-benzamido compound **15a** was approximately equipotent with **1** against PARP-2, but the increased bulk of the benzoyl group and loss of the basicity of the amine diminished the inhibition of PARP-1 dramatically, leading to a 9.3-fold selectivity toward inhibition of PARP-2. Exploration of the SAR around the phenyl ring indicated that introducing a para-substituent reduced the selectivity, mostly through decreasing the potency against PARP-2 (**15b**,**d**−**f**) rather than by increasing the inhibition of PARP-1; the 4-nitrobenzamido and 4-iodobenzamido analogues **15c**,**h** were the exception, where the compounds were more potent against PARP-1 than was **15a**. Moving the methyl group to the ortho-position of the benzamide, in **15i**, reduced inhibition against both isoforms, but the corresponding ortho-iodo compound **15j** was nonselective but had fairly good potency against PARP-1 and PARP-2.

dx.doi.org/10.1021/jm1010918 |J. Med. Chem. 2011, 54, 2049–2059

Table 1. Inhibition of the Activities of PARP-1 and PARP-2 by 5-Amidoisoquinolin-1-ones 15a−n and 22, by 5-(ω-Carboxyalkyl)- and 5-(ω-Carboxyalkylamino)isoquinolin-1-ones 24, 26, and 29, and by 2-(2-Carboxyethyl)isoquinolin-1-one 32[a]

	isoquinolinone		IC_{50} (μM)		
compd	3-substituent	5-substituent	PARP-1	PARP-2	observed selectivity ($IC_{50(PARP-1)}/(IC_{50(PARP-2)}$)
1	H	H_2N-	0.94 ± 0.10	1.05 ± 0.11	0.9
15a	H	PhCONH-	13.9 ± 1.2	1.5 ± 0.2	9.3
15b	H	4-MePhCONH-	13.4 ± 1.2	6.5 ± 0.8	2.1
15c	H	4-O_2NPhCONH-	3.0 ± 0.4	1.6 ± 0.2	1.9
15d	H	4-F_3CPhCONH-	10.7 ± 1.5	3.3 ± 1.0	3.2
15e	H	4-FPhCONH-	18.0 ± 1.2	3.6 ± 0.4	5.0
15f	H	4-ClPhCONH-	11.2 ± 1.3	3.9 ± 0.3	2.9
15g	H	4-BrPhCONH-	ND[b]	ND[b]	
15h	H	4-IPhCONH-	7.6[c]	1.3[c]	5.8
15i	H	2-MePhCONH-	31.6 ± 3.4	5.6 ± 0.4	5.6
15j	H	2-IPhCONH-	4.5 ± 1.2	3.2 ± 1.0	1.4
15k	H	(thiophen-2-yl)CONH-	22.4 ± 3.4	7.0 ± 1.2	3.2
15l	H	cHexCONH-	>80	27.9 ± 4.5	>2.9
15m	H	^{t}BuCONH-	>100	29 ± 3.4	>3.4
15n	H	(adamantan-1-yl)CONH-	>50	19.9 ± 3.0	>2.5
22	Me	PhCONH-	16.6 ± 1.2	6.3 ± 0.3	2.6
24	H	HO_2C-	>25	>25	
26	H	$HO_2CHC{=}HC$-	6.6 ± 1.0	4.7 ± 0.4	1.4
27	H	$HO_2CCH_2CH_2$-	8.6 ± 1.1	3.0 ± 0.2	2.9
29	H	HO_2CCH_2NH-	1.6 ± 0.1	0.55 ± 0.1	2.9
32[d]	H	H_2N-	0.55 ± 0.1	1.6 ± 0.3	0.4
10	H	$PhCO_2$-	4.1 ± 0.5	1.5 ± 0.4	2.75
9b	[2-(4-ClPh)quinoxaline-5-$CONH_2$]		0.03 ± 0.006	0.09 ± 0.02	0.33

[a] Data for **1**, 5-benzoyloxyisoquinolin-1-one **10**, and 2-(4-chlorophenyl)quinoxaline-5-carboxamide **9** are shown for comparison. [b] Not determined owing to limited solubility. [c] Measured once only. [d] Also carries -$CH_2CH_2CO_2H$ at the 2-position.

The common medicinal chemical replacement of a benzene ring with a thiophene, in **15k**, reduced potency against both isoforms, and replacement with bulky aliphatic groups, in **15l−n**, continued the trend of diminishing activity without gain of selectivity. Adding a methyl group at the 3-position, in **22**, caused loss of potency against PARP-2 relative to that of **15a** but retention of activity against PARP-1, leading to a loss of selectivity toward the former enzyme.

Curiously, the benzoate ester **10**, which is claimed to be the most selective for inhibition of PARP-2 with a reported ratio of IC_{50} values of ∼60,[33] had activity against PARP-2 very similar to that of the close analogue, the benzamide **15a**, as expected, but proved to be potent in our assay of inhibition of PARP-1 catalytic activity, giving a selectivity ratio of only 2.75. The quinoxaline-5-carboxamide **9b** was remarkably potent against both isoforms, with IC_{50} = 30 nM vs PARP-1 and IC_{50} = 90 nM vs PARP-2. These values give an approximate 3-fold selectivity for inhibition of PARP-1, in contrast to the claimed 5-fold selectivity for PARP-2.[39] These marked differences in apparent selectivities for the different isoforms probably arise from the different assays used and different sources of the enzymes used. Pellicciari et al.[33] compared bovine PARP-1 with murine PARP-2 using the incorporation of radioactivity from ^{3}H-NAD^+ into trichloroacetic acid-insoluble material as an assay of enzymic activity, whereas Iwashita et al.[39] compared human PARP-1 with murine PARP-2 using the same method.[60] We compared human PARP-1 with murine PARP-2 using different assay methods. Thus, it is highly likely that our comparative assays are a much more stringent test of selectivity for inhibition of PARP-2 than the assay pairs previously used or, alternatively, tend to bias toward reporting selectivity for inhibition of PARP-1.

Table 2. Inhibition of Growth of HT29 Human Colon Carcinoma Cells, MDA-MB-231 Human Breast Carcinoma Cells, LNCaP Human Prostate Carcinoma Cells, and FEK4 Human Dermal Fibroblast Cells by 1 and Selected 5-Amidoisoquinolin-1-ones 15a,l−n[a]

	IC_{50} (μM)			
compd	HT29	MDA-MB-231	LNCaP	FEK4
1	>200	170	>200	>200
15a	>200	139	98	>200
15l	>200	>200	>200	>200
15m	>200	>200	>200	>200
15n	>200	>200	42	>200

[a] Data are from single experiments using duplicates for each data point.

Table 1 also shows the evaluation of the isoquinolin-1-ones bearing a carboxy-terminated function at the 5-position. These carboxylates had been designed to interact with the positively charged side chain of Lys[308] near the PARP-2 NAD^+-binding site. By use of the current assays for PARP-1 and for PARP-2, isoquinolinone-5-carboxylic acid **24** showed little inhibition of

dx.doi.org/10.1021/jm1010918 |J. Med. Chem. 2011, 54, 2049–2059

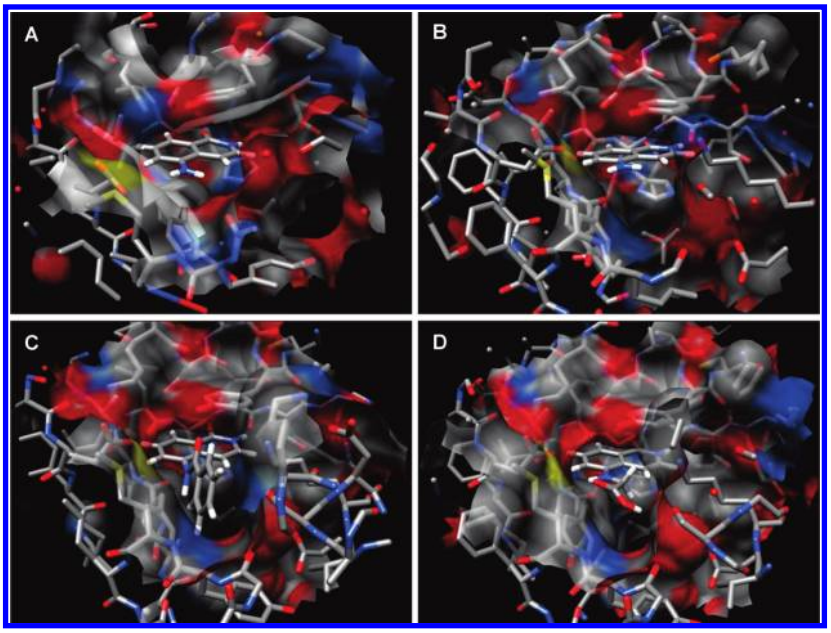

Figure 3. Modeling of the non-isoform-selective inhibitor **1** and the PARP-2-selective inhibitors **15a** and **29** into the NAD^+-binding sites of PARP-1 and PARP-2: (A) **1** in human PARP-1; (B) **1** in murine PARP-2; (C) **15a** in murine PARP-2; (D) **29** in murine PARP-2.

either isoform, a surprising result in view of the observation of $IC_{50} < 13\ \mu M$ in an earlier assay using broken cell nuclei as the source of PARP activity.[51] The isoquinolin-1-ones **26**, **27**, and **29** carrying the carboxy group attached to the 5-position through a more or less flexible linker were active against both isoforms but with modest selectivity. The isoquinolinone-5-propenoic acid had previously shown $IC_{50} < 11\ \mu M$ in the broken nuclei assay against mixed PARPs, broadly consistent with the presently observed values in the purified enzyme assays.[51] Curiously, **32**, which bears the carboxy group attached through a tether to the 2-N of the ring system, was potent against both isoforms, with ~3-fold selectivity for inhibition of PARP-1 over PARP-2. This compound appears to be slightly more potent against PARP-1 than is the lead PARP inhibitor **1** but lacks the N−H generally taken[3] to be part of the essential pharmacophore for binding to the PARPs (through an H-bond to Gly^{863}-O in PARP-1 and to Gly^{405}-O in PARP-2), but Eltze et al. have recently reported some inhibitors of PARP lacking this N−H (fused 2,3-dihydroquinolin-4-ones **5**, thus with CH_2 replacing the usual NH).[35] The precise binding mode of **32** to the PARPs will be the subject of later studies.

The most selective inhibitor of PARP-2 identified in our study, 5-benzamidoisoquinolin-1-one **15a**, together with the non-isoform-selective lead inhibitor **1** and examples **15l**−**n** of 5-(bulky alkyl)amidoisoquinolin-1-ones, which are poorly active against both isoforms, were evaluated for cytotoxicity toward a panel of three diverse human carcinoma cell lines and one human fibroblast cell line in vitro using the MTS colorimetric assay. None of the isoquinolin-1-ones were active against HT29 human colon carcinoma cells or the FEK4 normal human fibroblasts (Table 2). Two compounds, **1** and the most selective PARP-2 inhibitor **15a**, were very weakly cytotoxic toward the MDA-MB-231 human breast carcinoma cells, and two, **15a** and **15n**, were weakly cytotoxic toward the LNCaP human prostate carcinoma cells. These results are consistent with our previous observation that **1** caused only 40% inhibition of the proliferation of CT26 murine colon carcinoma cells at the very high concentration of 1 mM.[57] None of the cell lines used here have mutant BRCA, so the lack of cytotoxicity is unsurprising.

POST FACTO STRUCTURAL STUDIES

Post facto molecular modeling studies were undertaken to rationalize the strong selectivity for inhibition of PARP-2 observed for the 5-benzamidoisoquinolin-1-one **15a** and for the smaller but significant selectivity observed for the carboxylic acid **29**. These represent the most isoform-selective examples from each of the two series originally designed. These post facto studies were aided by the disclosure in 2009 (after the current experimental work had been completed) of a crystal structure of human PARP-1[58] and in 2010 of a crystal structure of human PARP-2 complexed with ABT888 **4**.[59] Starting structures were taken from published X-ray crystallographic structures of human PARP-1 complexed with a quinoxalinone inhibitor (A861696)[58] and of murine PARP-2 without an inhibitor ligand.[48] The latter was compared with the more recent data for human PARP-2 obtained with 3-aminobenzamide bound;[59] this comparison was used to drive docking and to refine the nicotinamide/inhibitor-binding pocket of PARP-2. Nonselective inhibitor **1** and PARP-2-selective inhibitors **15a** and **29** were then docked into the models using the existing bound inhibitor (for PARP-1) and the docked inhibitor (for PARP-2) as templates. Once docked, the inhibitors were subjected to molecular mechanics and dynamics calculations to establish optimal docking conformations. During these calculations, the receptor was restrained to its original conformation. Lastly, both the inhibitors and binding pockets (radius 10 Å) were subjected to molecular dynamics and finally molecular mechanics calculations to give the final structures (Figure 3). The structures of **15a** and of **29** made the expected hydrogen-bonding contacts of the lactam with the Ser and Gly residues and π-stacks of the isoquinoline-1-one cores with Tyr^{907} (PARP-1) and Tyr^{449} (PARP-2).

Differences between the binding pockets of PARP-1 and PARP-2 can be observed from the models. The binding pocket

dx.doi.org/10.1021/jm1010918 |*J. Med. Chem.* 2011, 54, 2049–2059

in PARP-1 is smaller than that of PARP-2. Furthermore, the cavity that accepts groups attached to the 5-position of isoquinolin-1-ones is arranged essentially in plane with the bound **1** in PARP-2 but lies significantly above the plane of the bound ligand in PARP-1. This means that any bulky substituent in this position should lead to selectivity for binding to PARP-2 and inhibit binding to PARP-1. Compound **1** has a very small amino group in this location, which can easily be accommodated in both structures. By contrast, the 5-benzamido group in **15a** can only be accommodated by the larger and in-plane void of the PARP-2 structure and is sterically excluded by PARP-1 (Figure 3). Indeed, it was not possible to generate a corresponding model for binding of **15a** to PARP-1, owing to steric clash of the benzamide unit with the walls of the pocket. Now, the apparent SAR requirement for a benzamide in the 5-position, rather than an equivalent aliphatic amide, can be rationalized by the establishment of an additional aromatic π-stacking interaction onto a Tyr residue (Tyr^{438}) in the wall of the pocket in PARP-2. The structure of human PARP-2 contains a captive water molecule near the 3-amino group of the bound inhibitor 3-aminobenzamide, and it has been proposed that this mediates hydrogen bonding to the amine.[59] A similar water-mediated hydrogen bond to the 5-NH_2 could also be responsible, in part, for the good binding of **1** to both PARP-1 and PARP-2. The facility for hydrogen bonding (now to the secondary amide N−H) is retained in bound **15a**.

Similar docking/modeling of the less selective inhibitor **29** into the active site of murine PARP-2 was carried out. The above putative water-mediated hydrogen bond is also available in this structure (from the 5-NH). The side chain is located within the "in plane" pocket of the PARP-2 protein, although the π-stacking is, of course, not possible. The terminal carboxylate can also access the ammonium side chain of Lys^{308}. The smaller size and the flexibility of the side chain of **29** permit access to both the larger pocket of PARP-2 and the smaller pocket of PARP-1, leading to more modest isoform-selectivity than for **15a**.

CONCLUSIONS

In this paper, we report the design, synthesis, and biochemical evaluation of new 5-substituted isoquinolin-1-ones as selective inhibitors of PARP-2. Compounds were designed partly by modeling using the reported crystal structures of the catalytic NAD^+-binding sites of PARP-1 and PARP-2.[48,49] A new high-yielding synthesis of our lead PARP inhibitor **1** has been developed, which has the potential for large-scale preparations of this important compound to make it more economically available for biological and chemical studies. A Hurtley coupling to 2-methyl-3-nitrobenzoic acid **16** led directly to the isocoumarin **19**; conversion of **19** to the isoquinolin-1-one **20** and reduction of the nitro group provided a good route to **21**. Acylation of the exocyclic amines of **1** and **21** gave the corresponding 5-amidoisoquinolin-1-ones **15a**−**n** and **22** in good yields. Four isoquinolin-1-ones carrying carboxylates at the 5-position (linked directly to the ring or through tethers) were synthesized by hydrolysis of 5-cyanoisoquinolin-1-one **23**, by a Heck coupling to 5-iodoisoquinolin-1-one **25** or by chain-extension from the amine of **1**. Under strongly basic conditions, **1** was alkylated at the ring 2-N rather than at the exocyclic amine.

The isoform-selectivities of compounds **24**, **26**, **27**, and **29**, carrying carboxylates designed to bind electrostatically to basic Lys^{308} in the PARP-2 structure, which replaces neutral Gln^{763} in PARP-1, were disappointing. Reasonable potency against PARP-2 was observed for **26**, **27**, and **29**, but inhibition of PARP-1 activity was also strong. The modest selectivity was rationalized by post facto modeling studies.

The 5-amidoisoquinolin-1-ones were investigated as more hydrolytically stable analogues of the benzoate ester **10**, for which Pellicciari et al. claimed 60-fold selectivity for inhibition of PARP-2.[33,56] Of this series, the simple benzamide **15a**, the closest analogue of **10**, proved to be the most selective ($IC_{50(PARP-1)}/IC_{50(PARP-2)}$ = 9.3). In our comparative assays, **15a** had activity equal to that of **10** against PARP-2 but **10** was much more potent than was **15a** against PARP-1, leading to an observed selectivity of only 2.75-fold for **10**. Similarly, the quinoxaline-5-carboxamide **9b** showed a 3-fold selectivity for PARP-1 in our comparative assays, contrasting with a claimed 5-fold selectivity for PARP-2.[39] In light of these results, it is now evident from our direct comparisons that 5-benzamidoisoquinolin-1-one **15a** is the most isoform-selective inhibitor of PARP-2 reported to date. Post facto modeling studies rationalized the structural basis of the observed selectivity.

EXPERIMENTAL SECTION

General. NMR spectra were recorded on JEOL Delta 270 and Varian Mercury 400 spectrometers. Mass spectra were obtained using VG7070E and Bruker microTOF spectrometers. IR spectra were measured on a Perkin-Elmer RXI FTIR spectrometer. The stationary phase for chromatography was silica gel. All reactions were carried out at ambient temperature unless otherwise stated. Solvents were evaporated under reduced pressure. Melting points were determined using a Reichert-Jung Thermo Galen instrument and are uncorrected. Target compounds for biochemical evaluation were >95% pure, as shown by CHN combustion microanalyses (carried out at the School of Pharmacy, University of London) and TLC for novel compounds and by identity of mp and TLC for known compounds. Compound **12** was obtained from the Aldrich Chemical Co.

5-Aminoisoquinolin-1-one Hydrochloride (1). Compound **14** (1.6 g, 8.4 mmol) was stirred with Pd/C (10%, 1.0 g) in EtOH (120 mL) and aqueous HCl (9 M, 4 mL) under H_2 for 2 h. The suspension was then filtered through Celite. The Celite pad and residue were suspended in water (1000 mL) and heated. The hot suspension was filtered through a second Celite pad. Concentration of the filtrate and drying gave **1** (1.2 g, 71%) as white crystals: mp 248−252 °C (dec) (lit.[15] 250−260 °C (dec)).

1-Chloro-5-nitroisoquinoline (13). Aqueous HNO_3 (70%, 850 mg, 13.4 mmol) in concentrated H_2SO_4 (5 mL) was added dropwise to **12** (2.00 g, 12.2 mmol) in concentrated H_2SO_4 (10 mL) at 0−5 °C. The mixture was stirred at 0 °C for 2 h, then poured onto ice. The precipitate was collected, washed (H_2O), dried, and recrystallized (EtOAc/hexanes) to give **13** (2.34 g, 92%) as pale yellow crystals: mp 181−183 °C (lit.[61] mp 183−184 °C).

5-Nitroisoquinolin-1-one (14). Compound **13** (5.00 g, 24.0 mmol) was stirred at 100 °C in AcOH (100 mL) for 40 h. The cooled suspension was then poured onto ice. The solid was collected, washed (H_2O), and recrystallized (EtOH) to give **14** (3.74 g, 82%) as pale yellow crystals: mp 247−249 °C (dec) (lit.[15] mp 247−249 °C).

5-Benzamidoisoquinolin-1-one (15a). Compound **1** (50 mg, 0.25 mmol) was stirred with PhCOCl (39 mg, 0.28 mmol) in pyridine (2.0 mL) at 90 °C for 16 h. Evaporation and recrystallization (EtOAc) gave **15a** (57 mg, 86%) as an off-white solid: mp >310 °C (dec).

3-Methyl-5-nitroisocoumarin (19). 2-Bromo-3-nitrobenzoic acid **16**[62] (2.5 g, 10 mmol) and Cu powder (67 mg, 1.1 mmol) were added to pentane-2,4-dione (5.3 g, 53 mmol) and KO^{t}Bu (2.3 g,

20 mmol) in ^{t}BuOH (50 mL). The mixture was boiled under reflux for 16 h, then poured into H_2O (350 mL) and acidified with aqueous HCl (2 M). Extraction (Et_2O), evaporation, and chromatography (hexane/EtOAc 3:2) gave **19** (470 mg, 23%) as yellow crystals: mp 199−200 °C.

3-Methyl-5-nitroisoquinolin-1(2*H*)-one (20). A solution of **19** (470 mg, 2.3 mmol) in $MeO(CH_2)_2OH$ (100 mL) was saturated with NH_3, boiled under reflux for 4 h, then evaporated until 10 mL remained. The concentrate was stored at 4 °C for 16 h. The solid was collected, washed (H_2O, EtOH), and recrystallized (MeOH) to give **20** (320 mg, 68%) as bright yellow crystals: mp 231−232 °C (dec).

5-Amino-3-methylisoquinolin-1(2*H*)-one (21). Compound **20** (320 mg, 1.6 mmol) was heated with $SnCl_2$ (900 mg, 4.7 mmol) in EtOH (20 mL) at 70 °C for 4 h, then carefully poured into ice−water (200 mL). The suspension was made alkaline with aqueous NaOH, and the precipitate was filtered. Extraction of the filtrate (EtOAc), evaporation, and recrystallization (hexane, EtOAc) gave **21** (160 mg, 59%) as yellow crystals: mp 183−184 °C.

3-(1-Oxoisoquinolin-5-yl)propanoic Acid (27). Compound **26** (160 mg, 8.4 mmol) in EtOH (25 mL) and aqueous HCl (34%, 4 mL) was stirred vigorously with Pd/C (10%, 100 mg) under H_2 for 2 h. Filtration (Celite) and evaporation of the solvent from the filtrate gave **27** (1.1 g, 66%) as white crystals: mp 260−263 °C.

Ethyl 2-(1-Oxoisoquinolin-5-ylamino)acetate (28). Compound **1** (1.0 g, 4.4 mmol), ^{i}Pr$_2$NEt (1.4 g, 11 mmol), ethyl bromoacetate (885 mg, 5.3 mmol), and NaI (100 mg, 0.7 mmol) were stirred at 80 °C in DMF (60 mL) for 16 h. Evaporation and recrystallization (MeOH) gave **28** (121 mg, 19%) as pale buff crystals: mp 199−201 °C.

5-(Carboxymethylamino)isoquinolin-1-one Hydrochloride (29). Ester **28** (94.0 mg, 0.39 mmol) was boiled under reflux in aqueous HCl (6.0 M, 4.0 mL) for 3 h. Evaporation gave **29** (86 mg, 87%) as a pale amber solid: mp 275−280 °C (dec).

Crystal Data for 33. All data were collected at 150 K on a Nonius kappaCCD diffractometer. The structure was solved using SHELXS-97[63] and refined using full-matrix least-squares in SHELXL-97. $C_{12}H_{12}N_2O_3$, M = 232.24, λ = 0.710 73 Å, triclinic, space group = $P\bar{1}$ (No. 2), a = 7.7290(3) Å, b = 7.7930(3) Å, c = 9.2330(4) Å, α = 103.760(2)°, β = 93.294(2)°, γ = 94.054(2)°, U = 537.23(4) Å^3, Z = 2, D_c = 1.436 g cm^{-3}, μ = 0.105 mm^{-1}, $F(000)$ = 244. Crystal size = 0.25 mm × 0.25 mm × 0.10 mm, unique reflections = 2405 [R_{int} = 0.0494], observed ($I > 2\sigma(I)$) = 1503, data/restraints/parameters = 2405/1/160. Final R indices [$I > 2\sigma(I)$], $R1$ = 0.0547, $wR2$ = 0.1355; R indices (all data) = $R1$ = 0.1010, $wR2$ = 0.1589. Max peak/hole, 0.718 and −0.309 e Å^{-3}. Crystallographic data for **33** have been deposited at the Cambridge Crystallographic Data Centre: CCDC 781071. Requests for data should be addressed to CCDC, 12 Union Road, Cambridge CB2 1EZ, U.K.

PARP-1 Inhibition Assay. Compounds were assayed for inhibition of the catalytic activity of PARP-1 using the FlashPlate scintillation proximity assay previously developed at KuDOS.[55] Compounds were evaluated at eight different concentrations (0.75 nM to 1.5 μM + further concentrations to 10 μM if necessary) in triplicate, using full-length human PARP-1 (∼50 ng) isolated from HeLa cell nuclear extract. Compounds were dissolved in DMSO prior to addition to give a final concentration of 2% in the assay mixture, a concentration that had been shown to have no effect on the activity of the enzyme. Oligonucleotides 5′-ACTTGATTAGTTACGTAACGTTATGATTGA-3′/5′-TCAATCATAACGTTACGTAACTAATCAAGT-3′ were used as the DNA ligand. The concentration of NAD$^+$ was 5.0 μM. The reaction buffer was HEPES (1.0 M, 12.5 mL), $MgCl_2$ (1.0 M, 6.25 mL), KCl (3.0 M, 8.3 mL), dithiothreitol (77 mg), glycerol (propane-1,2,3-triol, 50 mL), NP-40 (50 μL) made up to 500 mL with Milli-Q water, then adjusted to pH 7.6 with aqueous KOH (3.0 M). Compounds were incubated with the enzyme for 10 min. Then the other components were added and the reaction was allowed to proceed for 45 min. Data were fitted using a logarithmic concentration scale to a dose-response curve using SigmaPlot 11; IC_{50} values were measured usually in two or three independent experiments, and the mean values are reported.

PARP-2 Inhibition Assay. Compounds were assayed for inhibition of the catalytic activity of PARP-2 using a method in which recombinant full-length murine PARP-2 protein (Alexis) (∼50 ng) was bound by a PARP-2-specific antibody in a 96-well white-walled plate. PARP-2 activity was measured following addition of ^{3}H-NAD$^+$ and DNA.[36] After washing, scintillant was added to measure the ^{3}H incorporated. Compounds were evaluated at eight different concentrations (0.75 nM to 1.5 μM + further concentrations to 10 μM if necessary) in triplicate. Compounds were dissolved in DMSO prior to addition to give a final concentration of 2% in the assay mixture, a concentration that had been shown to have no effect on the activity of the enzyme. Oligonucleotides 5′-ACTTGATTAGTTACGTAACGTTATGATTGA-3′/5′-TCAATCATAACGTTACGTAACTAATCAAGT-3′ were used as the DNA ligand. The concentration of NAD$^+$ was 2.5 μM. The reaction buffer was HEPES (1.0 M, 12.5 mL), $MgCl_2$ (1.0 M, 6.25 mL), KCl (3.0 M, 8.3 mL), dithiothreitol (77 mg), glycerol (propane-1,2,3-triol, 50 mL), NP-40 (50 μL) made up to 500 mL with Milli-Q water, then adjusted to pH 7.6 with aqueous KOH (3.0 M). Compounds were incubated with the enzyme for 10 min. Then the other components were added, and the reaction was allowed to proceed for 45 min. Data were fitted using a logarithmic concentration scale to a dose-response curve using SigmaPlot 11. IC_{50} values were measured usually in two or three independent experiments, and the mean values are reported.

■ ASSOCIATED CONTENT

Supporting Information. Synthetic procedures and spectroscopic data for **15b**−**n**, **22**, **24**, **26**, **31**, and **32**; spectroscopic data for **1**, **13**, **14**, **15a**, **19**, **20**, **21**, and **27**−**29**; biochemical and cell biological evaluation procedures; dose-response curves; and elemental combustion analytical data. This material is available free of charge via the Internet at http://pubs.acs.org.

■ AUTHOR INFORMATION

Corresponding Author

*Phone: +44 1225 386840. Fax: +44 1225 386114. E-mail: m.d.threadgill@bath.ac.uk.

Present Addresses

[||]Chemistry Research Laboratory, University of Oxford, 12 Mansfield Road, Oxford OX1 3TA, U.K.

[⊥]Department of Pharmacy and Pharmaceutical Sciences, Trinity College Dublin, College Green, Dublin 2, Ireland.

■ ACKNOWLEDGMENT

We thank Dr. Timothy J. Woodman (University of Bath) for many of the NMR spectra, Dr. Anneke Lubben (University of Bath) for the mass spectra, and Professor Rex M. Tyrrell (University of Bath, U.K.) for the kind gift of the FEK4 cells. We are very grateful to KuDOS Pharmaceuticals Ltd., Cancer Research UK, and the University of Bath for financial support. M. D.T., M.D.L., and A.S.T. are members of Cancer Research at Bath (CR@B).

■ ABBREVIATIONS USED

PARP-2, poly(ADP-ribose) polymerase 2; PARP-1, poly(ADP-ribose) polymerase 1; 5-AIQ, 5-aminoisoquinolin-1-one; ADP,

adenosine diphosphate ribose; NAD^+, nicotinamide adenine dinucleotide; PAR, poly(ADP-ribose); BRCA, breast cancer type 1 susceptibility protein; SSB, single-strand break; TRF2, telomeric repeat-binding factor 2; MNU, *N*-methyl-*N*-nitrosourea

REFERENCES

(1) Chambon, P.; Weill, J. D.; Mandel, P. Nicotinamide mononucleotide activation of new DNA-dependent polyadenylic acid synthesizing nuclear enzyme. *Biochem. Biophys. Res. Commun.* **1963**, *11*, 39–43.

(2) Rouleau, M.; Patel, A.; Hendzel, M. J.; Kaufmann, S. H.; Poirier, G. G. PARP inhibition: PARP1 and beyond. *Nat. Rev. Cancer* **2010**, *10*, 293–301.

(3) Woon, E. C. Y.; Threadgill, M. D. Poly(ADP-ribose)polymerase inhibition—where now? *Curr. Med. Chem.* **2005**, *12*, 2373–2392.

(4) Smith, S. The world according to PARP. *Trends Biochem. Sci.* **2001**, *26*, 174–179.

(5) De Murcia, G.; Ménissier-de Murcia, J. Poly(ADP-ribose) polymerase—a molecular nick-sensor. *Trends Biochem. Sci.* **1994**, *19*, 172–176.

(6) Langelier, M. F.; Servent, K. M.; Rogers, E. E.; Pascal, J. M. A third zinc-binding domain of human poly(ADP-ribose) polymerase-1 coordinates DNA-dependent enzyme activation. *J. Biol. Chem.* **2008**, *283*, 4105–4114.

(7) Schreiber, V.; Molinete, M.; Boeuf, H.; de Murcia, G.; Ménissier-de Murcia, J. The human poly(ADP-ribose) polymerase nuclear localization signal is a bipartite element functionally separate from DNA binding and catalytic activity. *EMBO J.* **1992**, *11*, 3263–3269.

(8) Boulares, A. H.; Yakovlev, A. G.; Ivanova, V.; Stoica, B. A.; Wang, G.; Iyer, S.; Smulson, M. Role of poly(ADP-ribose) polymerase (PARP) cleavage in apoptosis. Caspase 3-resistant PARP mutant increases rates of apoptosis in transfected cells. *J. Biol. Chem.* **1999**, *274*, 22932–22940.

(9) Plummer, R.; Jones, C.; Middleton, M.; Wilson, R.; Evans, J.; Olsen, A.; Curtin, N.; Boddy, A.; McHugh, P.; Newell, D.; Harris, A.; Johnson, P.; Steinfeldt, H.; Dewji, R.; Wang, D.; Robson, L.; Calvert, H. Phase I study of the poly(ADP-ribose) polymerase inhibitor, AG014699, in combination with temozolomide in patients with advanced solid tumors. *Clin. Cancer Res.* **2008**, *14*, 7917–7923.

(10) Kummar, S.; Kinders, R.; Gutierrez, M. E.; Rubinstein, L.; Parchment, R. E.; Phillips, L. R.; Ji, J.; Monks, A.; Low, J. A.; Chen, A.; Murgo, A. J.; Collins, J.; Steinberg, S. M.; Eliopoulos, H.; Giranda, V. L.; Gordon, G.; Helman, L.; Wiltrout, R.; Tomaszewski, J. E.; Doroshow, J. H. Phase 0 clinical trial of the poly (ADP-ribose) polymerase inhibitor ABT-888 in patients with advanced malignancies. *J. Clin. Oncol.* **2009**, *27*, 2705–2711.

(11) Jones, P.; Altamura, S.; Boueres, J.; Ferrigno, F.; Fonsi, M.; Giomini, C.; Lamartina, S.; Monteagudo, E.; Ontoria, J. M.; Orsale, M. V.; Palumbi, M. C.; Pesci, S.; Roscilli, G.; Scarpelli, R.; Schultz-Fademrecht, C.; Toniatti, C.; Rowley, M. Discovery of 2-{4-[(3*S*)-piperidin-3-yl]phenyl}-2*H*-indazole-7-carboxamide (MK-4827): a novel oral poly(ADP-ribose)polymerase (PARP) inhibitor efficacious in BRCA-1 and-2 mutant tumors. *J. Med. Chem.* **2009**, *52*, 7170–7185.

(12) Gartner, E. M.; Burger, A. M.; LoRusso, P. M. Poly(ADP-ribose) polymerase inhibitors a novel drug class with a promising future. *Cancer J.* **2010**, *16*, 83–90.

(13) Fong, P. C.; Boss, D. S.; Yap, T. A.; Tutt, A.; Wu, P.; Mergui-Roelvink, M.; Mortimer, P.; Swaisland, H.; Lau, A.; O'Connor, M. J.; Ashworth, A.; Carmichael, J.; Kaye, S. B.; Schellens, J. H.; de Bono, J. S. Inhibition of poly(ADP-ribose) polymerase in tumors from BRCA mutation carriers. *N. Engl. J. Med.* **2009**, *361*, 123–134.

(14) Hay, T.; Matthews, J. R.; Pietzka, L.; Lau, A.; Cranston, A.; Nygren, A. O. H.; Douglas-Jones, A.; Smith, G. C. M.; Martin, N. M. B.; O'Connor, M.; Clarke, A. R. Poly(ADP-ribose) polymerase-1 inhibitor treatment regresses autochthonous *Brca2/p53*-mutant mammary tumors in vivo and delays tumor relapse in combination with carboplatin. *Cancer Res.* **2009**, *69*, 3850–3855.

(15) McDonald, M. C.; Mota-Filipe, H.; Wright, J. A.; Abdelrahman, M.; Threadgill, M. D.; Thompson, A. S.; Thiemermann, C. Effects of 5-aminoisoquinolinone, a water-soluble, potent inhibitor of the activity of poly(ADP-ribose)polymerase on the organ injury and dysfunction caused by haemorrhagic shock. *Br. J. Pharmacol.* **2000**, *130*, 843–850.

(16) Ferraris, D.; Pargas Ficco, R.; Dain, D.; Ginski, M.; Lautar, S.; Lee-Wisdom, K.; Liang, S.; Lin, Q.; Lu, M. X.-C.; Morgan, L.; Thomas, B.; Williams, L. R.; Zhang, J.; Zhou, Y.; Kalish, V. J. Design and synthesis of poly(ADP-ribose) polymerase-1 (PARP-1) inhibitors. Part 4: Biological evaluation of imidazobenzodiazepines as potent PARP-1 inhibitors for treatment of ischemic injuries. *Bioorg. Med. Chem.* **2003**, *11*, 3695–3707.

(17) Chatterjee, P. K.; Chatterjee, B. E.; Pedersen, H.; Sivarajah, A.; McDonald, M. C.; Mota-Filipe, H.; Brown, P. A. J.; Stewart, K. N.; Cuzzocrea, S.; Threadgill, M. D.; Thiemermann, C. 5-Aminoisoquinolinone reduces renal injury and dysfunction caused by ischaemia/reperfusion. *Kidney Int.* **2004**, *65*, 499–509.

(18) Hendryk, S.; Czuba, Z. P.; Jędrzejowska-Szypułka, H.; Szliszka, E.; Phillips, V. A.; Threadgill, M. D.; Król, W. Influence of 5-aminoisoquinolin-1-one (5-AIQ) on neutrophil chemiluminescence in rats with transient and prolonged focal cerebral ischaemia and after reperfusion. *J. Physiol. Pharmacol.* **2008**, *59*, 811–822.

(19) Cuzzocrea, S.; McDonald, M. C.; Mazzon, E.; Dugo, L.; Serraino, I.; Threadgill, M. D.; Caputi, A. P.; Thiemermann, C. Effects of 5-aminoisoquinolinone, a water-soluble potent inhibitor of the activity of poly(ADP-ribose) polymerase, in a rodent model of lung injury. *Biochem. Pharmacol.* **2002**, *63*, 293–304.

(20) Cuzzocrea, S.; Mazzon, E.; Di Paola, R.; Genovese, T.; Patel, N. S. A.; Muià, C.; Threadgill, M. D.; De Sarro, A.; Thiemermann, C. 5-Aminoisoquinolinone reduces colon injury by experimental colitis. *Naunyn-Schmiedeberg's Arch. Pharmacol.* **2004**, *370*, 464–473.

(21) Rajesh, M.; Mukhopadhyay, P.; Godlewski, G.; Bátkai, S.; Haskó, G.; Liaudet, L.; Pacher, P. Poly(ADP-ribose)polymerase inhibition decreases angiogenesis. *Biochem. Biophys. Res. Commun.* **2006**, *350*, 1056–1062.

(22) Li, M.; Threadgill, M. D.; Wang, Y.; Cai, L.; Lin, X. Poly(ADP-ribose) polymerase inhibition down-regulates expression of metastasis-related genes in CT26 colon carcinoma cells. *Pathobiology* **2009**, *76*, 108–116.

(23) Qin, Y.; Wang, Y.; Li, Y.-Y. Effect of poly(ADP-ribose)-polymerase inhibitor on the liver metastasis of mouse colorectal carcinoma CT-26 cell line *in vivo*. *J. Third Mil. Med. Univ.* **2008**, *30*, 1330–1333.

(24) Amé, J.-C.; Rolli, V.; Schreiber, V.; Niedergang, C.; Apiou, F.; Decker, P.; Muller, S.; Höger, T.; Ménissier-de Murcia, J.; de Murcia, G. PARP-2, A novel mammalian DNA damage-dependent poly(ADP-ribose) polymerase. *J. Biol. Chem.* **1999**, *274*, 17860–17868.

(25) Schreiber, V.; Amé, J.-C.; Dollé, P.; Schultz, I.; Rinaldi, B.; Fraulob, V.; Ménissier-de Murcia, J.; de Murcia, G. Poly(ADP-ribose) polymerase-2 (PARP-2) is required for efficient base excision DNA repair in association with PARP-1 and XRCC1. *J. Biol. Chem.* **2002**, *277*, 23028–23036.

(26) Fisher, A. E.; Hochegger, H.; Takeda, S.; Caldecott, K. W. Poly(ADP-ribose) polymerase 1 accelerates single-strand break repair in concert with poly(ADP-ribose) glycohydrolase. *Mol. Cell. Biol.* **2007**, *27*, 5597–5605.

(27) Dantzer, F.; Giraud-Panis, M. J.; Jaco, I.; Amé, J.-C.; Schultz, I.; Blasco, M.; Koering, C. E.; Gilson, E.; Ménissier-de Murcia, J.; de Murcia, G.; Schreiber, V. Functional interaction between poly(ADP-Ribose) polymerase 2 (PARP-2) and TRF2: PARP activity negatively regulates TRF2. *Mol. Cell. Biol.* **2004**, *24*, 1595–1607.

(28) Popoff, I.; Jijon, H.; Monia, B.; Tavernini, M.; Ma, M.; McKay, R.; Madsen, K. Antisense oligonucleotides to poly(ADP-ribose) polymerase-2 ameliorate colitis in interleukin-10-deficient mice. *J. Pharmacol. Exp. Ther.* **2002**, *303*, 1145–1154.

(29) Yélamos, J.; Monreal, Y.; Saenz, L.; Aguado, E.; Schreiber, V.; Mota, R.; Fuente, T.; Minguela, A.; Parrilla, P.; de Murcia, G.; Almarza, E.; Aparicio, P.; Ménissier-de Murcia, J. PARP-2 deficiency affects the survival of $CD4^+CD8^+$ double-positive thymocytes. *EMBO J.* **2006**, *25*, 4350–4360.

(30) Quéneta, D.; Mark, M.; Govin, J.; van Dorsseleard, A.; Schreiber, V.; Khochbin, S.; Dantzer, F. Parp2 is required for the differentiation of post-meiotic germ cells: identification of a spermatid-specific complex containing Parp1, Parp2, TP2 and HSPA2. *Exp. Cell Res.* **2009**, *315*, 2824–2834.

(31) Bai, P.; Houten, S. M.; Huber, A.; Schreiber, V.; Watanabe, M.; Kiss, B.; de Murcia, G.; Auwerx, J.; Ménissier-de Murcia, J. Peroxisome proliferator-activated receptor (PPAR)-2 controls adipocyte differentiation and adipose tissue function through the regulation of the activity of the retinoid X receptor/PPARg heterodimer. *J. Biol. Chem.* **2007**, *282*, 37738–37746.

(32) Yélamos, J.; Schreiber, V.; Dantzer, F. Toward specific functions of poly(ADP-ribose) polymerase-2. *Trends Mol. Med.* **2008**, *14*, 169–178.

(33) Pellicciari, R.; Camaioni, E.; Costantino, G.; Formentini, L.; Sabbatini, P.; Venturoni, F.; Eren, G.; Bellocchi, D.; Chiarugi, A.; Moroni, F. On the way to selective PARP-2 inhibitors. Design, synthesis, and preliminary evaluation of a series of isoquinolinone derivatives. *ChemMedChem* **2008**, *3*, 914–923.

(34) Penning, T. D.; Zhu, G.-D.; Gandhi, V. B.; Gong, J.; Liu, X.; Shi, Y.; Klinghofer, V.; Johnson, E. F.; Donawho, C. K.; Frost, D. J.; Bontcheva-Diaz, V.; Bouska, J. J.; Osterling, D. J.; Olson, A. M.; Marsh, K. C.; Luo, Y.; Giranda, V. L. Discovery of the poly(ADP-ribose) polymerase (PARP) inhibitor 2-[(*R*)-2-methylpyrrolidin-2-yl]-1*H*-benzimidazole-4-carboxamide (ABT-888) for the treatment of cancer. *J. Med. Chem.* **2009**, *52*, 514–523.

(35) Eltze, T.; Boer, R.; Wagner, T.; Weinbrenner, S.; McDonald, M. C.; Thiemermann, C.; Bürkle, A.; Klein, T. Imidazoquinolinone, imidazopyridine, and isoquinolindione derivatives as novel and potent inhibitors of the poly(ADP-ribose) polymerase (PARP): a comparison with standard PARP inhibitors. *Mol. Pharmacol.* **2008**, *74*, 1587–1598.

(36) Menear, K. A.; Adcock, C.; Boulter, R.; Cockcroft, X.-L.; Copsey, L.; Cranston, A.; Dillon, K. J.; Drzewiecki, J.; Garman, S.; Gomez, S.; Javaid, H.; Kerrigan, F.; Knights, C.; Lau, A.; Loh, V. M.; Matthews, I. T. W.; Moore, S.; O'Connor, M. J.; Smith, G. C. M.; Martin, N. M. B. 4-[3-(4-Cyclopropanecarbonylpiperazine-1-carbonyl)-4-fluorobenzyl]-2*H*-phthalazin-1-one: a novel bioavailable inhibitor of poly(ADP-ribose) polymerase-1. *J. Med. Chem.* **2008**, *51*, 6581–6591.

(37) Nakajima, H.; Kakui, N.; Ohkuma, K.; Ishikawa, M.; Hasegawa, T. A newly synthesized poly(ADP-ribose) polymerase inhibitor, DR2313 [2-methyl-3,5,7,8-tetrahydrothiopyrano[4,3-*d*]pyrimidine-4-one]: pharmacological profiles, neuroprotective effects, and therapeutic time window in cerebral ischemia in rats. *J. Pharmacol. Exp. Ther.* **2005**, *312*, 472–481.

(38) Ishida, J.; Yamamoto, H.; Kido, Y.; Kamijo, K.; Murano, K.; Miyake, H.; Ohkubo, M.; Kinoshita, T.; Warizaya, M.; Iwashita, A.; Mihara, K.; Matsuoka, N.; Hattori, K. Discovery of potent and selective PARP-1 and PARP-2 inhibitors: SBDD analysis via a combination of X-ray structural study and homology modeling. *Bioorg. Med. Chem.* **2006**, *14*, 1378–1390.

(39) Iwashita, A.; Mihara, K.; Yamazaki, S.; Matsuura, S.; Ishida, J.; Yamamoto, H.; Hattori, K.; Matsuoka, N.; Mutoh, S. A new poly(ADP-ribose) polymerase inhibitor, FR261529 [2-(4-chlorophenyl)-5-quinoxalinecarboxamide], ameliorates methamphetamine-induced dopaminergic neurotoxicity in mice. *J. Pharmacol. Exp. Ther.* **2004**, *310*, 1114–1124.

(40) Wenkert, E.; Johnston, B. D. R.; Dave, K. G. Derivatives of hemimellitic acid. A synthesis of erythrocentaurin. *J. Org. Chem.* **1964**, *29*, 2534–2542.

(41) Woon, E. C. Y.; Dhami, A.; Sunderland, P. T.; Chalkley, D. A.; Threadgill, M. D. Reductive cyclisation of 2-cyanomethyl-3-nitrobenzoates. *Lett. Org. Chem.* **2006**, *3*, 619–621.

(42) Berry, J. M.; Watson, C. Y.; Whish, W. J. D.; Threadgill, M. D. 5-Nitrofuran-2-ylmethyl group as a potential bioreductively activated prodrug system. *J. Chem. Soc., Perkin Trans. 1* **1997**, 1147–1156.

(43) Wong, S.-M.; Shah, B.; Shah, P.; Butt, I. C.; Woon, E. C. Y.; Wright, J. A.; Thompson, A. S.; Upton, C.; Threadgill, M. D. A new synthesis of "push−pull" naphthalenes by condensation of nitro-2-methylbenzoate esters with dimethylacetamide dimethyl acetal. *Tetrahedron Lett.* **2002**, *43*, 2299–2302.

(44) Serban, A. 3-Chloro-5-acetamidoisoquinoline as a herbicide. U.S. Patent 3930837, 1976

(45) Hurtley, W. R. H. Replacement of halogen in *ortho*bromobenzoic acid. *J. Chem. Soc.* **1929**, 1870–1873.

(46) Cirigottis, K. A.; Ritchie, E.; Taylor, W. C. Studies on the Hurtley reaction. *Aust. J. Chem.* **1974**, *27*, 2209–2228.

(47) Shinkwin, A. E.; Whish, W. J. D.; Threadgill, M. D. Synthesis of a series of thiophenecarboxamides, thieno[3,4-*c*]pyridin-4(5*H*)-ones and thieno[3,4-*d*]pyrimidin-4(3*H*)-ones and preliminary evaluation as inhibitors of poly(ADP-ribose)polymerase (PARP). *Bioorg. Med. Chem.* **1999**, *7*, 297–308.

(48) Oliver, A. W.; Amé, J.-C.; Roe, S. M.; Good, V.; de Murcia, G.; Pearl, L. H. Crystal structure of the catalytic fragment of murine poly(ADP-ribose) polymerase-2. *Nucleic Acids Res.* **2004**, *32*, 456–464.

(49) Ruf, A.; Ménissier de Murcia, J.; de Murcia, G.; Schulz, G. E. Structure of the catalytic fragment of poly(AD-ribose) polymerase from chicken. *Proc. Natl. Acad. Sci. U.S.A.* **1996**, *93*, 7481–7485.

(50) Ruf, A.; de Murcia, G.; Schulz, G. E. Inhibitor and NAD^+ binding to poly(ADP-ribose) polymerase as derived from crystal structures and homology modeling. *Biochemistry* **1998**, *37*, 3893–3900.

(51) Watson, C. Y.; Whish, W. J. D.; Threadgill, M. D. Synthesis of 3-substituted benzamides and 5-substituted isoquinolin-1(2*H*)-ones and preliminary evaluation as inhibitors of poly(ADP-ribose)polymerase (PARP). *Bioorg. Med. Chem.* **1998**, *6*, 721–734.

(52) Ferrer, S.; Naughton, D. P.; Parveen, I.; Threadgill, M. D. N- and O-Alkylation of isoquinolin-1-ones in the Mitsunobu reaction: development of potential drug delivery systems. *J. Chem. Soc., Perkin Trans. 1* **2002**, 335–340.

(53) Berry, J. M.; Threadgill, M. D. Labelled compounds of interest as antitumour agents. V. Syntheses of [^{18}O]-5-methylisoquinolinone and 1-(furan-2-yl-[^{18}O]-methoxy)-5-methylisoquinoline: Correction. *J. Labelled Compd. Radiopharm.* **1997**, *39*, 453 (Correction).

(54) Berry, J. M.; Threadgill, M. D. Labelled compounds of interest as antitumour agents. V. Syntheses of [^{18}O]-5-methylisoquinolinone and 1-(furan-2-yl-[^{18}O]-methoxy)-5-methylisoquinoline. *J. Labelled Compd. Radiopharm.* **1996**, *38*, 935–940.

(55) Dillon, K. J.; Smith, G. C. M.; Martin, N. M. B. A FlashPlate assay for the identification of PARP-1 inhibitors. *J. Biomol. Screening* **2003**, *8*, 347–352.

(56) Moroni, F.; Formentini, L.; Gerace, E.; Camaioni, E.; Pellegrini-Giampietro, D. E.; Chiarugi, A.; Pellicciari, R. Selective PARP-2 inhibitors increase apoptosis in hippocampal slices but protect cortical cells in models of post-ischaemic brain damage. *Br. J. Pharmacol.* **2009**, *157*, 854–862.

(57) Cai, L.; Threadgill, M. D.; Wang, Y.; Li, M. Effect of poly (ADP-ribose) polymerase-1 inhibition on the proliferation of murine colon carcinoma CT26 cells. *Pathol. Oncol. Res.* **2009**, *15*, 323–328.

(58) Miyashiro, J.; Woods, K. W.; Park, C. H.; Liu, X.; Shi, Y.; Johnson, E. F.; Bouska, J. J.; Olson, A. M.; Luo, Y.; Fry, E. H.; Giranda, V. L.; Penning, T. D. Synthesis and SAR of novel tricyclic quinoxalinone inhibitors of poly(ADP-ribose)polymerase-1 (PARP-1). *Bioorg. Med. Chem. Lett.* **2009**, *19*, 4050–4054.

(59) Karlberg, T.; Hammarström, M.; Schütz, P.; Svensson, L.; Schüler, H. Crystal structure of the catalytic domain of human PARP2 in complex with PARP inhibitor ABT-888. *Biochemistry* **2010**, *49*, 1056–1058.

(60) Banasik, M.; Komura, H.; Shimoyama, M.; Ueda, K. Specific inhibitors of poly(ADP-ribose) synthetase and mono(ADP-ribosyl)-transferase. *J. Biol. Chem.* **1992**, *267*, 1569–1575.

(61) Elpern, B.; Hamilton, C. S. Arsenicals in the isoquinoline series. *J. Am. Chem. Soc.* **1946**, *68*, 1436–1438.

(62) Sienkowska, M.; Benin, V.; Kaszynski, P. Preparation and NMR analysis of 2,6-heterodifunctional halobenzenes as precursors for substituted biphenyls. *Tetrahedron* **2000**, *56*, 165–173.

(63) Sheldrick, G. M. SHELXL-97, a Computer Program for Crystal Structure Refinement; University of Göttingen: Göttingen, Germany, 1997.